Appendix A

Harding Lawson Associates Report

This page is intentionally left blank.

GEOTECHNICAL INVESTIGATION REPORT
Subsurface Disposal Area Pits 4, 6 and 10, Idaho National Engineering and Environmental Laboratory Idaho Falls, ID

Prepared for

Lockheed Martin Idaho Technologies Company
P.O. Box 1625
Idaho Falls, ID 83415

HLA Project No. 46905

Prepared by

Nicholas E. Josten
Geophysical Analyst, GeoSense

Phil Meis, P.E.
Associate Engineer, HLA

August 10, 1999

Harding Lawson Associates
Engineering, Environmental & Construction
155 South 300 West, #103
Salt Lake City, UT 84101 - (801) 363-4455

TABLE OF CONTENTS

LIST OF FIGURES

LIST OF TABLES

1.0 INTRODUCTION

This report presents the results of the geotechnical investigation for Pits 4, 6 and 10 at the Idaho National Engineering and Environmental Laboratory's Subsurface Disposal Area.

1.1 Project Description

The subject geophysical investigation focuses on Pit 4, Pit 6 and Pit 10 (Pits 4-6-10) located near the center of the INEEL Subsurface Disposal Area (SDA) as shown in Figure 1. As the INEEL's principal buried hazardous waste facility, the SDA encompasses nearly 90 acres and contains 20 pits, 58 trenches, numerous engineered soil vaults, as well as buildings, roads and other infrastructure associated with management of the buried waste. The surface geophysical surveys and other remedial activities for Pits 4-6-10 are managed by INEEL under Operable Unit (OU) 7-13/14.

Pits 4-6-10 have an estimated average depth of 14.5 feet. Waste buried in these pits was generated primarily by weapons production operations at the DOE Rocky Flats Plant near Golden, CO and INEEL nuclear reactor testing activities. The sludge and other waste materials from Rocky Flats contain a variety of radionuclides, organic, and inorganic compounds. Other materials in Pits 4-6-10 include low-level waste from the INEEL and small quantities of low-level waste from miscellaneous off-site facilities.[1]

The geophysical investigation encompasses the historical locations of Pits 4-6-10. Table 1 lists the dimensions and area of these pits based on historical records. The actual geophysical survey covered approximately 9 acres in order to include non-waste areas between and around the pits (see Figure 1). Including these marginal areas is necessary to clearly image pit boundaries.

TABLE 1. PITS 4-6-10 DIMENSIONS.

Name	NS dimension (feet)	EW dimension (feet)	Area (sq ft)	Area (acres)
Pit 4	142	970	13,7740	3.16
Pit 6	117	490	57,330	1.32
Pit 10	133	1170	147,630	3.39
			342,700	7.87

The survey terrain was predominantly level, grassy field. Roadways bordered by drainage ditches cross the survey site at several locations. Fences, bollards, monitoring wells, piezometer installations, underground utilities, pipelines, barricades and various buildings were present throughout the site. These features produced local interference with geophysical measurements and are discussed further in a section below.

1.2 Objectives and Scope

[1] Waste inventory data taken from INEEL External Report No. INEEL/EXT-98-00856, Becker et. al., "Operable Unit 7-13/14 Plan for the Installation and Logging of Probeholes in Pits 4 and 10 of the Subsurface Disposal Area".

Objectives of the subject geophysical surveys were to locate pit boundaries, locate and characterize objects within pit boundaries, evaluate soil moisture distribution, and determine depth to basalt. The OU7-13/14 project will use the geophysical results to support planned intrusive waste sampling efforts. Planned future efforts include installation of cased probeholes, subsurface geophysical logging and core extraction. Geophysical data will be used, in combination with historical waste shipment records, to select probehole and core locations. In addition, soil conductivity and bedrock depth data will support soil treatment studies within Pits 4-6-10.

1.3 Consent of Authorization

Written authorization to proceed with the subject field investigation was provided to HLA in a fax dated April 14, 1999 from Bob Crowton of Lockheed Martin Idaho Technologies Company to Philip Meis of HLA.

2.0 GEOPHYSICAL METHODS

The geophysical program for Pits 4-6-10 consisted of high-density magnetic, electromagnetic and seismic refraction surveys. Table 2 lists target survey specifications.

TABLE 2. PITS 4-6-10 GEOPHYSICAL SURVEY SPECIFICATIONS

Method	Line spacing	Data spacing	Samples per 100 sq ft
Magnetic field	0.5 m	0.15 m	124
Transient electromagnetic	1.0 m	0.25 m	37
Frequency electromagnetic	1.0 m	0.50 m	19
Refraction seismic	15 m	2 m	1

2.1 Magnetics

Ground based magnetic surveys are used to measure spatial variations of the earth's magnetic field. Ferrous metal objects (i.e. iron and steel) cause localized distortions of the earth's magnetic field. These distortions are strongest near the object and fall off rapidly with distance. A magnetic survey detects these distortions, which are referred to as magnetic anomalies. Large objects such as 55 gallon drums can be detected from distances of 10 feet or more under low noise conditions.

Magnetic measurements are very selective in the sense that only highly ferrous materials create measurable magnetic field distortions. Iron and steel have exceptionally high ferrous material content and are readily detected by magnetic field measurements. Other metals (e.g. aluminum, lead, copper, etc.) contain no ferrous material and are invisible to the magnetic method. Common soils and rocks usually contain trace amounts of ferrous minerals but total ferrous content is normally small in comparison with the ferrous content of iron and steel objects. Basalt, which forms bedrock beneath the Pits 4-6-10 survey area, is an exception and can produce measurable magnetic anomalies. In most cases basalt related anomalies have a distinct character that permits the interpreter to recognize and differentiate them from anomalies caused by metal objects. In difficult cases, complementary electromagnetic data sets may be used to make this distinction.

In addition to being highly selective, the magnetic method has the highest sensitivity and best spatial resolution of the common metal detecting geophysical methods. Spatial resolution is further enhanced by use of magnetic gradient measurements, wherein two magnetometers are used to measure the changes in magnetic field over short distances. Magnetic gradient methods have the property of rejecting magnetic anomalies from more distant sources in favor of anomalies from nearby sources and are normally more useful for buried waste applications. HLA collected both magnetic field and magnetic gradient measurements at Pits 4-6-10.

2.2 Transient Electromagnetics

The electromagnetic induction method operates by creating a time varying magnetic field, which causes electric eddy currents to flow in nearby conductive objects. The induction instrument then measures the secondary magnetic fields associated with these eddy currents. As with the magnetic method, the secondary magnetic fields fall off rapidly with distance, but objects such as 55 gallon drums can be detected over nearly the same range as for magnetic field mapping systems.

In transient electromagnetic methods, the instrument generates a current pulse in a transmitter coil to produce the time varying primary magnetic. The transmitter current reaches maximum amplitude and is abruptly terminated many times per second, producing the inductive effect in nearby objects. Induced currents in low conductivity materials (e.g. soil and rock) dissipate rapidly, but induced currents in high conductivity materials persist for longer periods. The instrument's receiver detects the gradual decay of these persistent eddy currents only, which accounts for the utility of the tool as a metal detector. Because the transient instrument is insensitive to soil/rock conductivity, and because the primary magnetic field is turned off during measurement of eddy current decay, transient electromagnetic induction instruments produce clean, low noise measurements even under varying soil conditions.

The Geonics EM61 instrument used for the Pits 4-6-10 survey has two receiver coils, designated upper and lower. This coil arrangement permits calculation of a differential response similar to the vertical gradient measurement in magnetics. The EM61's internal processor applies numerical corrections to the differential calculation that result in rejection of shallow sources in favor of deep sources.

2.3 Multi-frequency Electromagnetics

The principle of frequency based induction instruments is identical to transient instruments except that the time varying primary field is a continuous sinusoidal waveform rather than a pulsed waveform. This primary field induces sinusoidal electric current flow in nearby conductive materials. The instrument receiver measures the sinusoidally varying magnetic field associated with current flow. Instrument response is resolved into two components - an in-phase component related primarily to high conductivity materials such as metallic objects, and a quadrature component related primarily to low conductivity materials such as soil and rock. The quadrature component provides information not obtainable from conventional transient induction instruments.

Frequency based induction instruments are inherently noisy due to the fact that the primary field is continuously active and has a very large amplitude compared with the secondary field. Most instruments incorporate a balancing coil that is used to counteract the primary field effects and improve signal to noise characteristics.

A multi-frequency induction instrument generates a primary field "sweep" over a range of frequencies. Lower frequencies provide greater depth of investigation. Thus a multi-frequency instrument offers variable depth of investigation. However, investigation depth also depends on other factors such as target conductivity, soil conductivity and target orientation. Since these factors are normally unknown, precise investigation depth is not easily quantified (Witten et. al. 1997) but frequency may still be used as a general depth indicator[2].

[2] Witten A., I.J. Won and S. Norton, 1997, "Imaging Underground Structures Using Broadband Electromagnetic Induction", JEEG, Vol 2, No 2, pp 99 -104, Engineering and Environmental Geophysics Society, Wheatridge, CO.

2.4 Seismic Refraction

Seismic refraction is used to determine the depth and configuration of bedrock and to estimate fill and overburden thickness. Seismic refraction can also provide information about the weathering and excavation characteristics of the bedrock. Seismic refraction surveys entail measuring the compressional (P) wave velocity of earth materials using an array of detectors (geophones) embedded into the ground. P-wave energy is usually generated by a sledgehammer blow or small explosive charge. P-wave energy traveling through the subsurface is detected by the geophones and signals from the geophones are fed into a seismograph, which stores the data in memory. The seismograph can also output data in the field to support quality control and preliminary interpretation.

Seismic data are output as seismograms, which are plots of ground motion versus time at each geophone location. A hammer blow or explosion generates elastic waves that shake the geophones as they propagate through the ground. The shaking motion is recorded as deflections in the seismic traces. Because the P-wave is the fastest traveling seismic wave, it can be identified as the first sharp downward departure ("break") from horizontal on a seismic trace. Vibrations from nearby machinery and vehicles or from wind can produce noise on the seismic records and make P-wave arrivals difficult to identify. If noise levels are too high first breaks cannot be picked accurately, causing erroneous interpretations of subsurface conditions.

The P-wave velocity depends on the compaction, density, and/or hardness of earth materials (i.e. soil and rock). Since these parameters generally increase with depth, seismic velocity also increases with depth, in most cases. The seismic velocity of rock is inversely proportional to the degree of weathering. That is, more deeply weathered the rock will exhibit a lower seismic velocity than less weathered and unweathered rock.

Some general correlations between velocity and rock type are recognized. Bedrock with little fracturing or weathering typically has seismic velocities of greater than 10,000 feet per second (fps). Weathered bedrock and lithified sediments often have seismic velocities ranging from 3,000 fps to 9,000 fps. Unconsolidated sediment, alluvium, and landfill materials typically have seismic velocities ranging from 800 fps to 2,500 fps.

Seismic velocity can also vary laterally. In general, lateral velocity variations are produced by lateral changes in weathering, lithification, fracturing, or composition of soil, fill, and rock. Geologic phenomena such as the presence of faults and shear zones are often responsible for lateral velocity variations. In addition, cultural features such as grading, compacting, and landfilling can cause lateral velocity variations.

By recognizing and accounting for these factors during the evaluation of seismic refraction data one can make some general and specific interpretations about subsurface conditions.

3.0 FIELD INVESTIGATION

The boundary of the Pits 4-6-10 geophysical investigation is shown in Figure 1. In general, the investigation area comprised the accessible portion of the landfill cap above the pits and the areas immediately adjacent to the pit boundaries.

3.1 Description of Investigation Area

The topography of the landfill cap is predominantly level with a slight runoff crown. At the time of the investigation, the cap was lightly vegetated with wheat grass and small sagebrush. Roadways bordered by drainage ditches dissected the investigation area in many places, and an active disposal pit was operating in the eastern portion of the study area.

Numerous surface obstructions, including fences, bollards, monitoring wells, piezometer installations, above ground pipelines, concrete barricades, storage containers, and several buildings were present at the time of the investigation. In addition, site included three radiological control areas - the area around the two SVE process buildings, and the entire east end of the study area at the active disposal pit. Geophysical data could not be obtained in several places, most notably, at the radiological control zones, near the above ground piping, and near the land/sea storage containers.

3.2 Survey Grid Layout

A site walk was performed to inspect the survey area prior to grid layout and data acquisition. HLA observed that a 24- by 30-foot control grid had been installed previously throughout much of the Pit 10 area and over a portion of the Pit 4 area. Mr. Dave Burgess (LMITCO) informed HLA that the grid had been installed for a soil gas survey and that X Y coordinates for the grid points had been recorded and could be used for the geophysical survey. Consequently, HLA requested that the specifications for the geophysical survey grid be changed from the proposed metric system to the English system that was already in place. Mr. Bruce Becker (LMITCO) approved HLA's request, effectively changing the grid layout from the 2 m by 10 m grid, as was originally proposed, to a 6 ft by 30 ft grid. It followed that survey line spacing would change from 0.5 m and 1 m, to 1.5 ft and 3 ft, respectively. After verifying the dimensions of the existing grid, HLA used a fiberglass tape measure and PVC pin flags to expand the existing Pit 10 control grid to include the entire geophysical investigation area. Because HLA noticed a slight location shift in the soil gas grid in the Pit 4 area, all horizontal control for the geophysical data was referenced to the Pit 10 soil gas survey control grid.

The southwest corner of the survey grid was set as the survey origin (0 East, 0 North) and the pin flags along each base line were labeled accordingly (Figure 2). The survey grid area measured a maximum of 306 feet wide in the north-south direction and a maximum of 1350 feet long in the east-west direction. PVC pin flags were placed at 6-foot intervals along north-south lines spaced 30 feet apart except within the radiological control areas, which could not be surveyed due to access restrictions. The grid arrangement facilitated data acquisition along east-west trending survey transects with a distance reference point every 30 feet. Additionally, tall wood lathe were staked at 150-foot intervals along the 0 North, 144 North, and 288 North survey lines, providing coarse index grid to help the field crew quickly determine locations during data acquisition.

3.3 Site Features Mapping

After the survey grid was installed, HLA used a total station survey instrument to record the locations of the numerous cultural features that restricted survey access or would create sources of geophysical noise. The feature locations and geophysics survey grid stake locations were tied to the known survey coordinates at the disposal pit corners. In general, HLA surveyed the locations of surface metal objects, underground utility markers, exclusion zones, and drainage features. In addition, the HLA geophysicist prepared a hand-drawn site map of the investigation area. The location of roads, drainage features, concrete barricades, and subsidence features were plotted on this map using the installed survey grid for reference. The primary purpose of the site map was to document the presence of features affecting the survey coverage, as well as the presence and location of features that might affect the geophysical measurements themselves. The total station survey data and the hand-drawn site features map were compiled into a single site features map (Figure 2).

3.3 Data Acquisition

3.4.1 Magnetic Survey

Magnetic data were acquired using a Geometrics 858 (G-858) cesium-vapor magnetometer / gradiometer operated in the vertical magnetic gradient configuration. In the gradient configuration, the G-858 instrument obtains total magnetic field data from two sensors simultaneously. The two sensors were mounted 2.5 vertical feet apart at the end of a staff, with the lower sensor approximately 1.5 feet above the ground surface. By using the simultaneously obtained data, the true vertical gradient of the earth's magnetic field can be computed by subtracting the lower sensor from the upper sensor reading. These values are then scaled by the separation distance to provide the vertical magnetic gradient in nanoTeslas (nT) per foot.

Magnetic data were obtained by hand-carrying the G-858 along east-west trending survey transects spaced 1.5 feet apart. The data were obtained at a rate of 10 readings per second (a 0.1 second recording interval). Survey speed was limited to approximately 4 feet per second to maintain an average data spacing of no greater than 0.6 ft per reading. Line numbers (grid northing distances) were entered into the instrument memory by the operator. Distance along each line is automatically recorded by the instrument through use of fiducial marks entered at 30-foot intervals at the pin flag locations.

In addition to the G-858 field magnetometer, a G-856 proton precession magnetometer was used as a base station to record the naturally occurring diurnal variations in the earth's magnetic field. The base station data was used to remove diurnal variations from the total field data. The base station magnetometer was set in the same location each day and data were acquired at 30-second intervals throughout the field data acquisition periods.

3.4.2 Transient Electromagnetic (EM61) Survey

Transient EM data were collected using a Geonics EM61 in the towed cart configuration. The EM61 is a two coil (horizontal, coaxial) metal detecting EM system, designed for high spatial resolution applications. The two coils are mounted on wheels and are separated vertically by approximately 16 inches. The lower (main) coil operates approximately 16 inches above the ground surface and the upper (focussing) coil operates approximately 32 inches above the ground surface. Evaluation of the

simultaneously obtained upper- and lower-coil EM data can provide burial depth information, and allows for the enhanced discrimination of closely-spaced buried objects.

The EM61 was hand towed along each survey transect. EM61 data were obtained along east-west trending survey transects spaced 3 feet apart. The data were acquired at four readings per second (a 0.25 second interval). Survey speed was limited to approximately 3 feet per second to maintain an average data spacing of approximately 0.8 ft. The geophysicist entered line numbers (grid northing distance) into instrument memory, and distances along each line were automatically recorded by the instrument through use of fiducial marks, which were entered at 30-foot intervals at the pin flag locations.

3.4.3 Frequency Electromagnetic (GEM-300) Survey

Multi-frequency EM data were collected using a GEM-300. The GEM-300 is a two coil (horizontal, coplanar) EM system designed for high spatial resolution and depth sensitive applications. The GEM-300 was operated in the vertical dipole, in-line survey mode with an instrument height of 3.5 feet above the ground. The instrument was set to obtain both quadrature and in-phase data from 4 frequencies between 450 Hz to 19950 Hz. The suite of frequencies was intended to maximize target resolution and investigation depth. Selectable GEM-300 frequencies are factory programmed for half-multiples of 60 Hz. A low frequency of 450 Hz was selected as the lowest frequency producing data of acceptable quality. A high frequency of 19950 Hz was selected because it was the highest available frequency that is a half multiple of 60 Hz. The instrument was allowed to auto-select the intermediate frequencies at geometrically spaced intervals between 450 Hz and 19950 Hz, resulting in operating frequencies of 450 Hz, 1590 Hz, 5610 Hz, and 19950 Hz. The factory null calibration was used as an absolute reference for all measurements.

The GEM-300 was hand carried along east-west trending survey transects spaced 3 feet apart. The data were acquired at eight readings per second (a 0.125 second interval) for four frequencies, which was analogous to obtaining two readings for each frequency every 1 second. Survey speed was limited to approximately 3 feet per second to maintain an average data spacing of approximately 1.6 feet per reading. Line numbers (grid northing distance) were entered into instrument memory by the operator. Distances along each line were automatically recorded by the instrument through use of fiducial marks, entered by the operator at 30-foot intervals at the pin flag locations.

3.4.4 Seismic Refraction Survey

The seismic refraction data were acquired using a 24-channel Geometrics SmartSeis instantaneous floating point seismograph and Mark Products, Inc., 14-Hz digital geophones. Seismic energy was generated by repeatedly striking a 16-pound sledge hammer against a metal plate placed on the ground at each shotpoint location. The resulting P-waves were detected using collinear arrays (spreads) of 24 geophones coupled to the ground at 6-foot intervals. Shotpoints were located 6 feet beyond each end point of every spread, and in the middle of each spread. The resulting seismic spreads were 150 feet long. Sixty (60) seismic spreads were obtained resulting in 8,100 feet of refraction data. A hand-level was used to measure topographic variations along the seismic lines, and also to measure the difference in ground surface elevation between the 60 seismic spreads.

To maximize seismic data coverage, HLA distributed the sixty 150-foot long seismic spreads in a "checkerboard" fashion across the investigation area. In general, 300-foot-long north-south trending lines consisting of two seismic spreads were positioned at 60-foot intervals across the site. HLA also obtained refraction data along two east-west tie lines positioned along the axis of the disposal pits, at grid

lines 102 N and 240 N. Two shorter tie lines were positioned at grid lines 120 N and 276 N, where access along the primary tie lines was limited (see Figure 2).

Seismograms for each shotpoint were output in the field as the survey progressed. The geophysicist used the seismograms for preliminary field interpretations to insure that the data were of acceptable quality and to verify that bedrock was detected. The seismograms were evaluated for the quality of the first breaks, and for matching reciprocal end times. As a further check, preliminary velocity layer and bedrock depth models were produced in the field using the SmartSeis' seismic interpretation program. The HLA geophysicist observed that the data quality was highly variable, ranging from excellent to poor, owing in large part to high noise levels and the quality of the subsurface materials.

The primary noise sources were wind energy and ground vibrations caused by the motors and compressors of the SVE system. In addition, the absorptive properties of the poorly consolidated landfill cap and disposal materials, including possible void spaces within the landfill cells, effected both the input and transmission of seismic energy. Where present the combination of high noise levels and poor energy transmission reduced the signal-to-noise ratio and severely affected data quality. The geophysicist boosted signal strength by stacking (adding) multiple hammer blows at each shot point, although in some cases the noise levels were so high that the signal-to-noise ratio remained poor.

3.5 Data Processing

3.5.1 Magnetic and electromagnetic data processing

Data processing for the magnetic and electromagnetic data sets consisted of four basic steps: 1) local x,y coordinate reduction, 2) bias removal, 3) delay correction and 4) conversion to global coordinates. Reduction to local x,y, coordinates converts raw measurement values to scaled coordinates in the survey reference frame, with the origin located in the SW corner of the survey area. Bias removal is necessary because electromagnetic data (and particularly multi-frequency electromagnetic data) have a tendency to drift caused by changing battery condition and charge buildup in electronic components. During bias removal, the data are adjusted to a common background level. For magnetic data, bias removal corrects for the naturally occurring diurnal drift in the earth's magnetic field strength. The drift is measured by a fixed base station that collects data simultaneously with survey data. Delay corrections account for finite instrument response time, which causes data point locations to shift slightly towards the surveying direction during data acquisition. Alternating lines are collected by walking in opposite directions and the delay shift generates a herringbone effect in uncorrected data. Delay corrections reduce this effect and improve the appearance of the mapped data. After preliminary processing, data are converted to a global coordinate system as specified by LMITCO. Details for this coordinate system are provided in Appendix B.

3.5.2 Seismic data processing

ISeismic refraction data processing entails picking the first break arrival times from the seismograms and then preparing a TD graph of arrival time versus distance for all geophones and shotpoints in a given spread or set of spreads. Guided by the graphs, the geophysical analyst uses a computer program to develop a model of subsurface velocity layering; specifically, the models depict the number of velocity layers, their thickness, and their average velocity. The analyst then correlates the velocity layering to geologic layering.

Interpretation of the seismic refraction data was finalized using a computer program that calculates an average velocity for each layer and depths to the refracting surfaces. The input to the program includes horizontal and vertical positions of all shotpoints and geophones, first arrival times for each geophone, and layer designations for each arrival time as determined from the TD graphs. In reducing the seismic data, the program uses velocity calculation and ray-tracing procedures to calculate a seismic model that fits the observed data. The computer program output consists of a graphical profile depicting subsurface velocity layering, and tables listing the computed average velocity and the depth to each seismic layer beneath every shotpoint and geophone. The bedrock depth information was then input into a computer-contouring software program to produce a bedrock depth contour map.

Three assumptions are made during the reduction of seismic refraction data and the validity of these assumptions largely governs the applicability of the refraction method and the accuracy of the subsurface models. These assumptions are a) the subsurface consists of relatively flat lying (less than 20 degrees from the horizontal) within the geophone spread, b) the P-wave velocity is continuous within each layer, and c) the layer velocities increase with depth. The seismic refraction method cannot provide detailed information about local variations in material velocity and rock condition. Rather, the velocity models represent average velocity for each layer.

3.6 Mapping

After processing, geophysical data are interpolated onto a regular grid. Gridded data may then be displayed in various graphical forms such as contour maps, color intensity maps and shaded relief maps. The map displays are the basis for subsequent interpretation. Final map displays are presented in Plates 1 - 8 as designated in Table 3.

TABLE 3. GEOPHYSICAL MAP DISPLAYS.

Figure	Content
Plate 1	Total field magnetics
Plate 2	Vertical gradient magnetics
Plate 3	Transient EM - lower coil
Plate 4	Transient EM - differential
Plate 5	Multi-frequency EM - 450 Hz
Plate 6	Multi-frequency EM - 1590 Hz
Plate 7	Multi-frequency EM - 5610 Hz
Plate 8	Multi-frequency EM - 19950 Hz

4.0 FINDINGS

4.1 Pit Boundary Interpretation

Disposal operations commonly depend almost exclusively on steel drums (or other metal containers) for hazardous waste packaging and these drums constitute an excellent target for geophysical investigation. Magnetic and transient electromagnetic data are the principal tools for mapping the extent of buried metallic objects in the subsurface. Because the drums are typically packed closely together and buried in pits, the limits of metallic waste may be used as an estimate of pit boundary locations. However, the data are insensitive to any non-metallic materials that may be present in the subsurface. Pit boundary interpretations should be used with caution where non-metallic waste is suspected.

Figure 3 shows the interpreted limits of metallic waste within and around Pits 4-6-10 based on magnetic and transient electromagnetic data. This figure also shows the historical boundary location of Pits 4-6-10 for comparison. The historical pit locations are seen to be generally accurate with local exceptions. The geophysical data show multiple buried objects adjacent to the southwest Pit 10 boundary and extending for approximately 100 feet beyond. In three locations - 100 ft west of the NE Pit 4 corner, 350 east of the NW Pit 10 corner, and 50 feet east of the southern Pit 10 corner - buried metal objects or object groups clearly extend beyond the historical pit boundaries. In other areas, interpreted limits of metal waste occur close to and locally intersect the historical boundary, but the overlap may be attributable to uncertainty in interpreting the exact waste edge from geophysical data.

The geophysical data show clear no-waste margins surrounding the Pits 4-6-10 complex except along the southwest boundary of Pit 10. The no-waste margin along the southern boundary of Pit 10 is relatively narrow compared with other boundaries, particularly adjacent to Pit 13 (compare Figure1). Locations of trenches and/or individual soil vaults are readily discernible north of Pits 4 and 6 (compare Figure 1). Buried metal materials appear to be more continuously distributed toward the eastern end of the trench/soil vault rows than on the western end. This continuous distribution is more evident in the magnetic data than the transient EM data, and it is possible that basalt related magnetic anomalies contribute to the appearance of continuous disposal. Integrating geophysical data with historical information concerning the trench/soil vaults may permit a clearer interpretation.

The boundary between Pits 4 and 6 has virtually no geophysical expression. A slight decrease in the measured transient EM response across the historical boundary suggests that the type, amount, or depth of buried materials changes near this boundary. Nonetheless, the distribution of buried materials appears to be continuous across the boundary.

Locations of geophysical anomalies indicative of numerous shallow or surface metal objects are shown as red crosses in Figure 3. These geophysical anomalies may be caused by surface debris, monuments, well heads or other man-made structures. The Pits 4-6-10 site contained numerous obstructions and buried utilities, the most prominent of which are shown on Figure 3 (compare also Figure 2). These structures have strong geophysical signatures and create local blind zones that cannot be evaluated for the presence of buried objects.

4.2 Pit Sub-boundaries and Waste Block Interpretation

Figure 4 shows an interpretation of sub-boundaries within Pits 4-6-10. Sub-boundaries are drawn based on qualitative variations in geophysical signature. The observed variations suggest the presence of separate waste blocks. Buried materials within separate waste blocks may have contrasting physical character, container types, container distribution patterns, depth, date of disposal, or other properties. The waste block interpretation offers a possible link with historical disposal records.

Table 4 gives a descriptive summary of waste block characteristics. The waste block interpretation is based on patterns of amplitude change in the geophysical data.. Decreased amplitude can result either from increased burial depth or lower buried metal content. While it is not possible to determine between these possibilities with any certainty, waste records may provide additional information on which to refine the waste block characterization.

TABLE 4. PITS 4-6-10 WASTE BLOCK CHARACTERISTICS.

Waste block	Approx area (acres)	Characteristics
Block A	0.95	High metal content and/or thinner overburden throughout; north-south groupings predominate; row of buried materials along southern boundary
No waste zone	0.08	No geophysical evidence for buried metal; possible basalt high based on magnetics, seismic refraction
Block B	1.20	Metal content decreases and/or overburden thickens from west to east; north-south groupings predominate;
Block C	0.73	Lower metal content and/or thicker overburden; row of buried materials along southern boundary
Block D	0.55	Lower metal content and/or thicker overburden; two large anomalies show isolated buried masses along southern boundary
Block E	1.69	High metal content and/or thin overburden; north-south groupings of Block A and B not evident; composed of smaller, more randomly distributed groupings
Block F	0.20	Lower metal content and/or thicker overburden
Block G	0.10	Isolated north-south trend indicating locally high metal content and/or thin overburden
Block H	0.60	Lower metal content and/or thicker overburden similar to Block H

4.3 Conductivity and Magnetization Trends

In general, the purpose of conductivity and magnetization trend analysis is to identify and assess changes in shallow soil and rock characteristics. For example, increased soil conductivity may indicate the presence of elevated soil moisture or changes in pore fluid conductivity. Magnetization changes are

caused by variation in soil/rock iron mineral content and may be used to identify lithology changes. Soil/rock conductivity and magnetization cannot ordinarily be evaluated at landfill sites such as Pits 4-6-10 due to the predominant influence from buried metal objects. Metal objects have magnetization and conductivity values many orders of magnitude higher than typical soils and rocks. The Pits 4-6-10 geophysical data were analyzed on a limited basis restricted to the overburden and local areas having low metal content. A summary of this analysis is presented in Figure 5. Interpreted conductivity and magnetization trends should be used cautiously due to the prevalent influence of metal related signals.

The multi-frequency electromagnetic data were the primary basis for conductivity analysis. Under natural soil/rock conditions, the instrument's quadrature component response may be calibrated directly to produce apparent conductivity values. At sites containing buried metal the quadrature response becomes "contaminated" by the influence of metallic objects, but can still indicate elevated soil conductivity in a qualitative fashion.

Two types of conductivity features are mapped in Figure 5. Broad low conductivity areas were identified from the low frequency (450 Hz) data, which has the greatest depth of investigation. These areas may be caused by high stands of electrically resistive bedrock basalt. The low conductivity area crossing the northern boundary of Pit 4 corresponds with a no-waste zone and it possible that this area contained insufficient soil depth for waste burial.

Numerous high conductivity zones were identified based on the high frequency (19950 Hz) data. The high frequency data reflect conductivity variation in the uppermost 5 - 10 feet of soil. It is likely that the mapped high conductivity zones correspond with increased shallow soil moisture. Several topographic depressions were identified during field operations at the exact location of conductivity highs (compare Figure 2). The high conductivity zones could also be influenced by fluids at greater depths, including fluids associated with buried waste. A review of historical disposal records may help to establish this relationship. Figure 5 also shows the location of roadways and shallow buried utility lines, which were clearly detectable in the 19950 Hz data set.

Total field magnetic data were used to evaluate signatures from bedrock basalt. Several apparent high magnetization trends are shown in Figure 5 based on subtle changes in the background magnetic field. The features may be associated with basalt high stands or locally increased basalt magnetization. Basalt magnetization is a highly variable parameter, changing both horizontally and vertically between boundaries of individual lava flows.

4.4 Depth Analysis

4.4.1 Seismic Refraction

A contour map showing the depth to basaltic bedrock is shown Figure 6. In general, the refraction data indicate that bedrock ranges in depth from 3 feet to 41 feet below ground surface (bgs), with bedrock over most of the site between 15 and 25 feet bgs. The findings correspond well with reports that the basaltic bedrock beneath Pits 4-6-10 ranges from 11 feet to 26 feet bgs, and that the average depth of the disposal pits is approximately 14.5 feet bgs. Some general trends are apparent: bedrock is shallower towards the west end of the investigation area than toward the east and the bedrock surface displays a pattern of roughly parallel, north-south ridges and depressions. This pattern may reflect basalt flow features. The bedrock ridge crossing beneath the middle of Pit 4 correlates with magnetic and EM indications of shallow basalt (compare Figure 5).

While interpreting the refraction data, HLA considered a conceptual framework for SDA site that consisted of from 2 to 4 seismically identifiable layers. The two-layer case would be soil directly overlying bedrock; this is the simplest case and is not observed in the refraction data. Several different three-layer cases are possible - soil over alluvium over bedrock, landfill cap over landfill debris over bedrock, or landfill debris over alluvium over bedrock. Finally, at least one four-layer case also exists - landfill cap over landfill material over alluvium over bedrock.

While a close examination of the TD graphs showed a few possible two-layer cases and a very marginal four-layer case, the seismic refraction data generally indicated a geologic model consisting of three velocity layers. The upper layer (layer V1) was generally a very slow material with velocities ranging from 800 feet per second (fps) to 1,300 fps, with the majority of V1 velocities grouped around 900 fps. Layer V1 ranges in thickness from 0 ft to 20 ft and is interpreted to represent the landfill cover or poorly consolidated landfill debris. It is generally associated with the areas of fine-grained silty cap material. Although this is shown as locally discontinuous it is not possible to distinguish cap material from landfill debris in areas where the velocities are similar. The intermediate layer (layer V2) has velocities ranging from 1,200 fps to 1,850 fps. Layer V2 ranges in thickness from 0 ft to 38 ft and is interpreted to represent landfill debris and poorly consolidated alluvium. The bottom layer (V3) shows velocities ranging from 4,000 fps to 8,000 fps. Layer V3 ranges in depth from 3 ft to 41 ft below ground surface (bgs) and is interpreted to represent the top of the weathered basalt. The broad velocity range for layer V3 is thought to represent variations in the nature of basalt – its composition, texture, and associated weathering characteristics.

4.4.2 Magnetics and Electromagnetics

Empirical depth estimation techniques have been widely used in magnetic data analysis since about 1950[3]. These methods were originally developed by the petroleum industry for interpreting sedimentary basin depths but have more recently been adapted for use in shallow geotechnical applications[4]. The depth estimate method is based on measuring the horizontal extent of the steep magnetic gradient that occurs over the edge of a magnetized subsurface body. The measured gradient extent is related to the object depth by an empirically determined calibration factor. Harding Lawson Associates/GeoSense have developed calibration factors applicable to landfill sites for both magnetic total field and magnetic vertical gradient data.

Empirical depth estimation methods using transient EM data have been developed by instrument manufacturers. These methods also depend fundamentally on measuring the width of measured anomalies. Calibration factors are included in software supplied with the instrument and cannot be adjusted.

Under low noise circumstances, depth estimation techniques for landfill sites are generally accurate to within ± 30% of the estimated depth. Estimation techniques assume that geophysical anomalies are caused by single, isolated sources and are susceptible to errors when applied to complex anomalies caused by multiple objects at various depths. Landfill sites produce few truly isolated anomalies, which degrades depth estimate accuracy. Nonetheless, useful results can usually be obtained by careful selection of anomalies for depth analysis.

---

[3] Vacquier, V. and N.C. Steenland, R.G. Henderson, and I. Zietz, 1951, Interpretation of Aeromagnetic Maps: Geologic Society of America Memoir 47, New York, NY.

[4] Josten, N. E., 1995, Progress on Development of the Dig-face Characterization Technology, Lockheed Idaho Technologies Company Report No. INEL-95/0093, Idaho National Engineering laboratory, Idaho Falls, ID.

Figure 7 shows results from depth-to-waste analysis of Pits 4-6-10 magnetic and electromagnetic data. The individual depth estimate locations are plotted along with the approximate depth or depth range (where more than one estimate was made). Minimum, maximum and average depths for each pit are given in Tables 5 and 6.

TABLE 5. DEPTH TO METALLIC OBJECTS BASED ON MAGNETIC DATA DEPTH ESTIMATES.

Pit	Number of estimates	Minimum depth (ft)	Maximum depth (ft)	Average depth (ft)
4	21	2.8	14.2	6.7
6	7	4.5	12.8	7.2
10	33	3.6	17	7.7

TABLE 6. DEPTH TO METALLIC OBJECTS BASED ON ELECTROMAGNETIC DATA DEPTH ESTIMATES.

Pit	Number of estimates	Minimum depth (ft)	Maximum depth (ft)	Average depth (ft)
4	22	2.8	8.9	6.9
6	4	6.8	10.5	8.3
10	21	2.3	7.5	5.8

Tables 5 and 6 show considerable depth variation, which undoubtedly reflects actual variation in object depth as well as uncertainty associated with the estimation techniques. Few objects were found to have depths less than four feet and the great majority have depths between 6 and 8 feet. This depth range may serve as an estimate for average overburden depth throughout Pits 4-6-10.

5.0 CONCLUSIONS AND RECOMMENDATIONS

5.1 Conclusions

The primary conclusions from the Pits 4-6-10 geophysical program may be restated as follows:

- Magnetic and EM data reveal the widespread presence of buried metallic objects in the subsurface of Pits 4-6-10.
- Geophysical data show the historical Pit 4-6-10 boundaries to be generally accurate with exceptions as noted below
- Geophysical data show no evidence for a boundary between Pits 4 and 6
- Magnetic and EM data show a large group of buried objects in the subsurface extending for approximately 100 feet beyond the southwest boundary of Pit 10
- The historical northern boundaries of Pits 4-6-10 appear to be tight boundaries, i.e. subsurface objects occur close to and possibly slightly beyond the historical position
- In a few locations adjacent to Pits 4 and 10, isolated objects (or object groups) occur clearly outside the historical boundary
- Broad changes in geophysical data characteristics suggest the presence of separate waste blocks within Pits 4-6-10, which may reflect changes in historical disposal practices
- Magnetic and EM conductivity data show the possible location of basalt ridges that correspond with areas having relatively sparse subsurface metal objects; the location of an apparent ridge near the center of Pit 4 is corroborated by seismic refraction data
- EM data show areas with high conductivity soils within the waste overburden that may be due to increased soil moisture within small, local topographic depressions
- Basalt depth beneath Pits 4-6-10 varies between <10 ft and greater than 30 ft, with a roughly north-south pattern of ridges and depressions
- Average depth to metallic waste is estimated at 6 ft to 8 ft for most of Pits 4-6-10, with local indications that objects may occur as shallow as 3 ft.

5.2 Recommendations

The high density geophysical data collected at Pits 4-6-10 contain a great deal of detailed information with which to address specific remedial design questions as they arise. Superior spatial resolution make these data ideal for future integration with historical records. The following recommendations are offered for future use of these data:

- In choosing future drilling, sampling or other instrusive activity sites, the geophysical data should be evaluated on a small scale, as maps and individual data profiles, to take full advantage of the inherent resolution of these data sets
- Depth to basalt interpretation may be improved by integrating the seismic refraction data with all available well data within or surrounding Pits 4-6-10

6.0 PROFESSIONAL STATEMENTS

This document was prepared for the sole use of Lockheed Martin Idaho Technolgies Company, the only intended beneficiary of our work. No other party should rely on the information contained herein without the prior written consent of HLA.

Supporting data upon which geotechnical conclusions and recommendations are based are presented in Appendix A. Conclusions and recommendations presented here are governed by assumed physical properties of the soils, bedrock, and buried waste materials within and around Pits 4-6-10. If subsurface conditions other than those described in this report are encountered during subsequent drilling or excavations, it may become necessary to revise some conclusions.

Our professional services have been performed, our findings obtained, and our recommendations prepared in accordance with generally excepted engineering principles and practices at this time.

Figure 1. Site map.

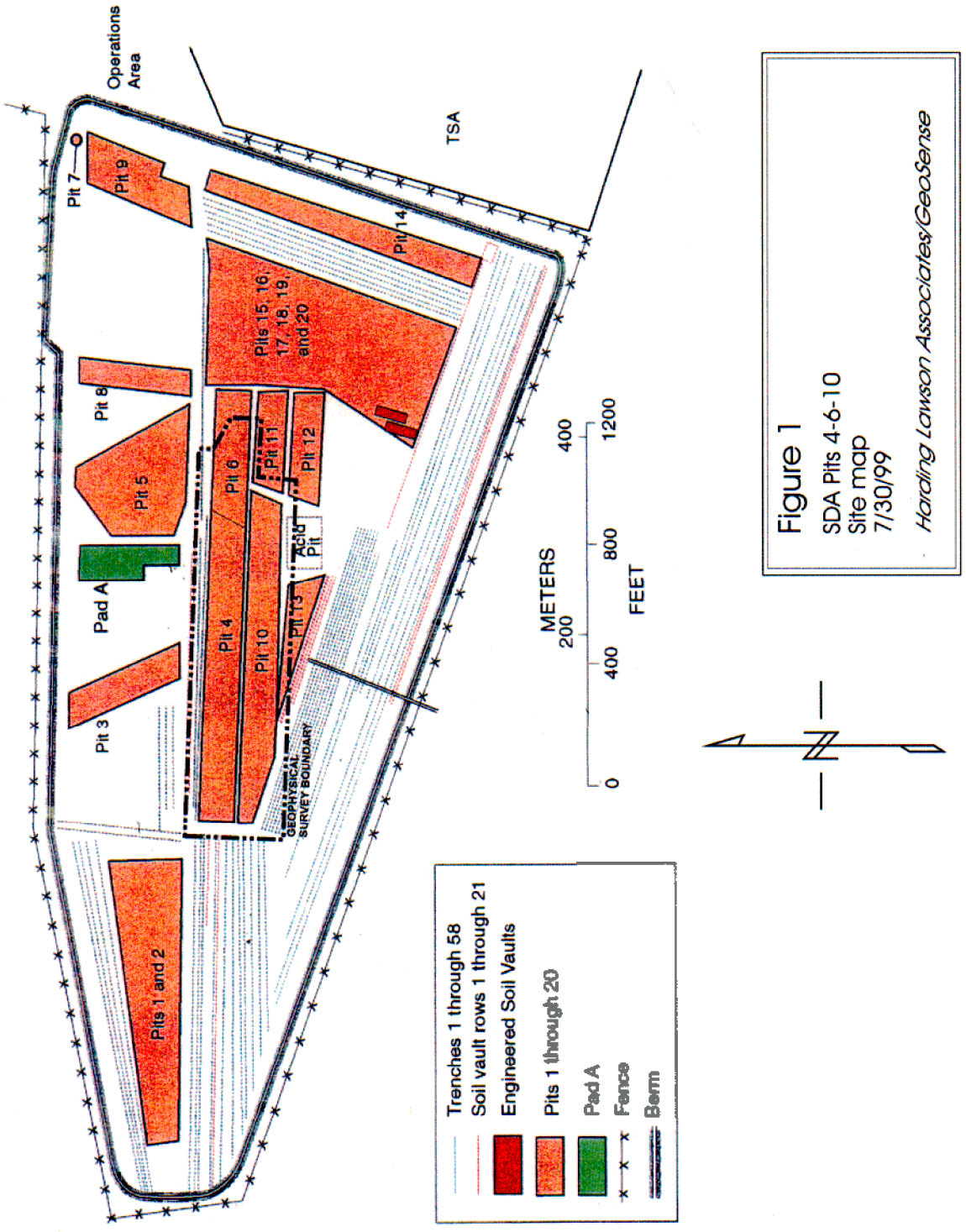

Figure 2. Site features map.

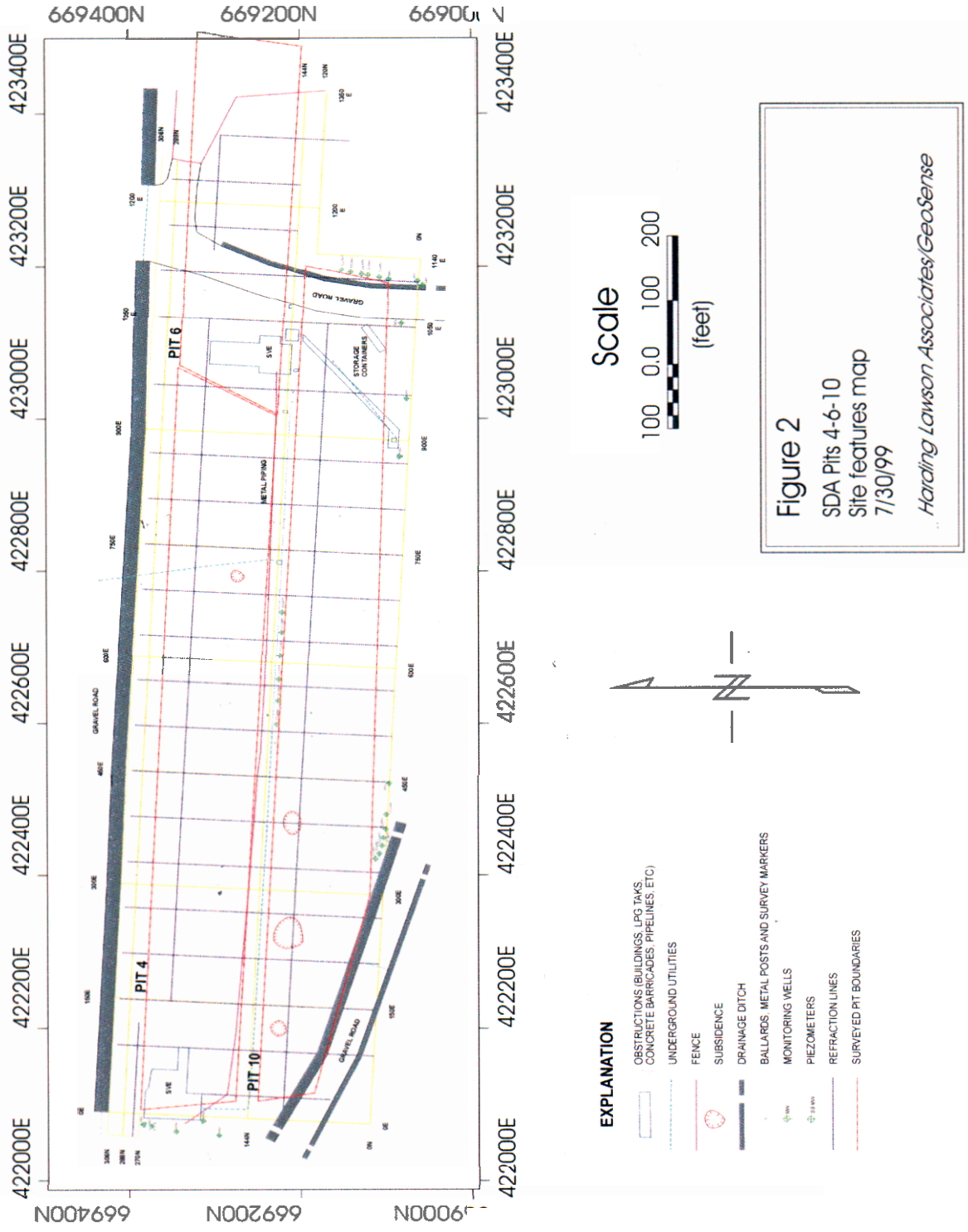

Figure 3. Pit boundary interpretation.

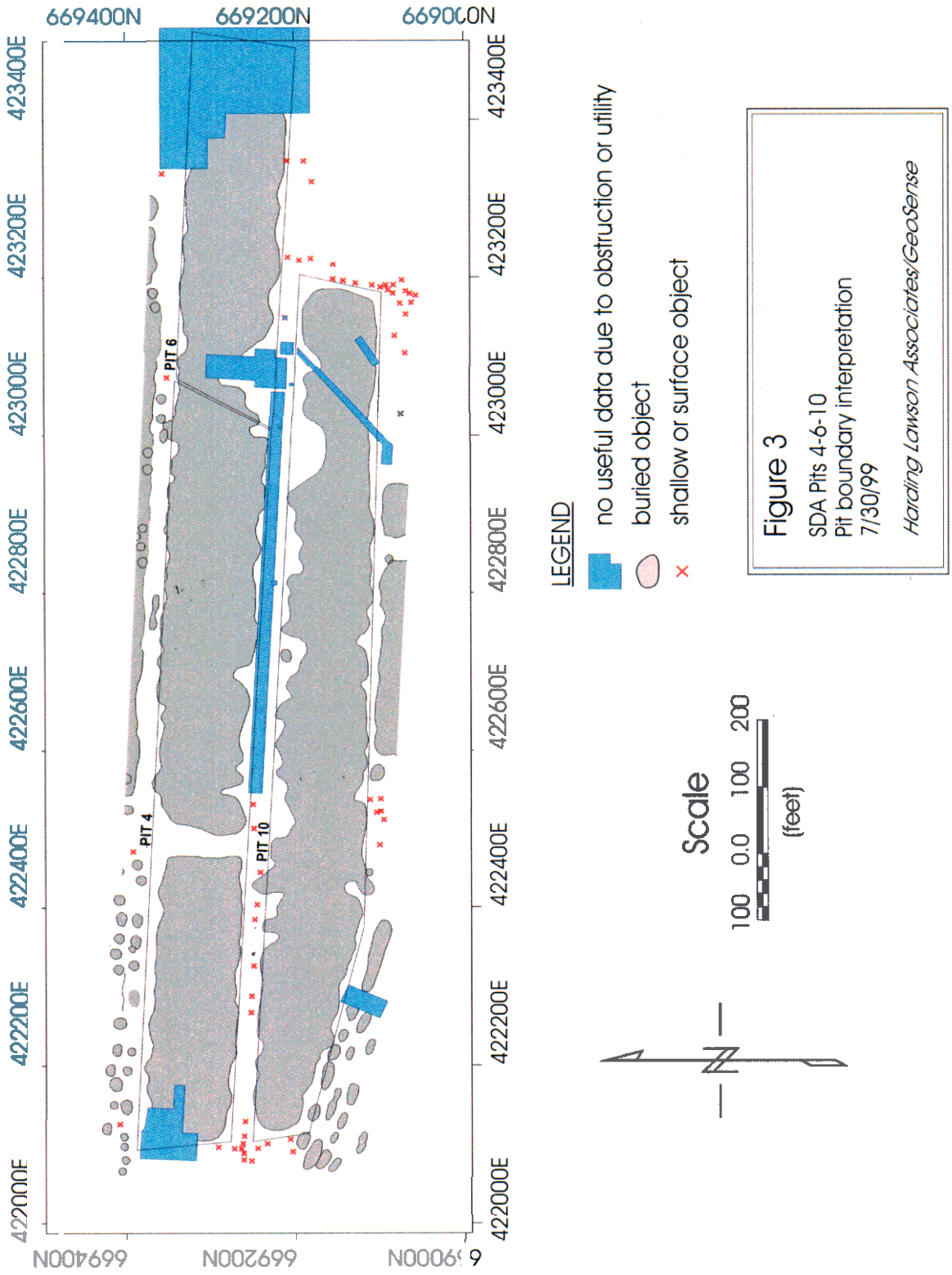

Figure 4. Waste block boundary interpretation.

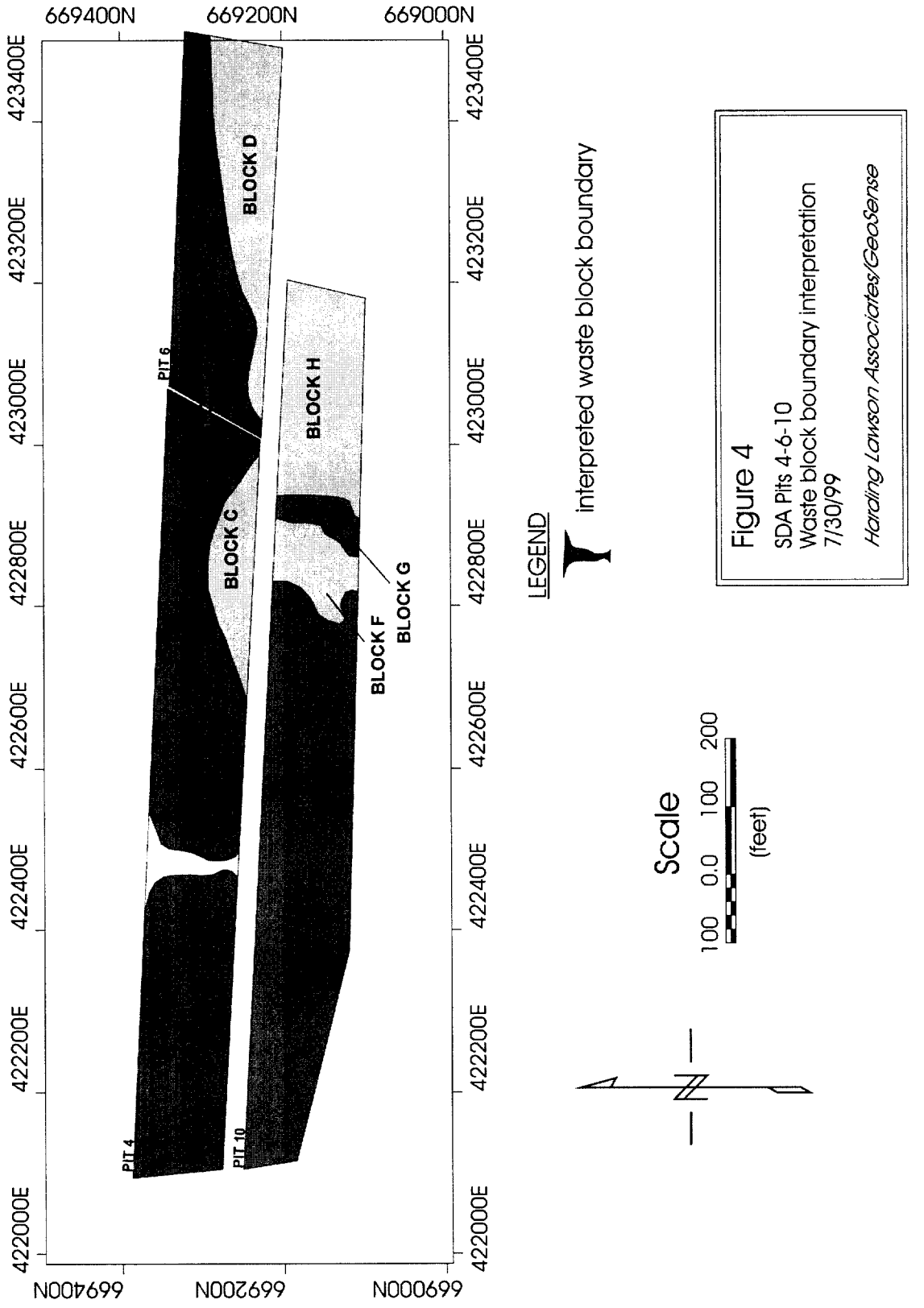

Figure 5. Conductivity and magnetization trends.

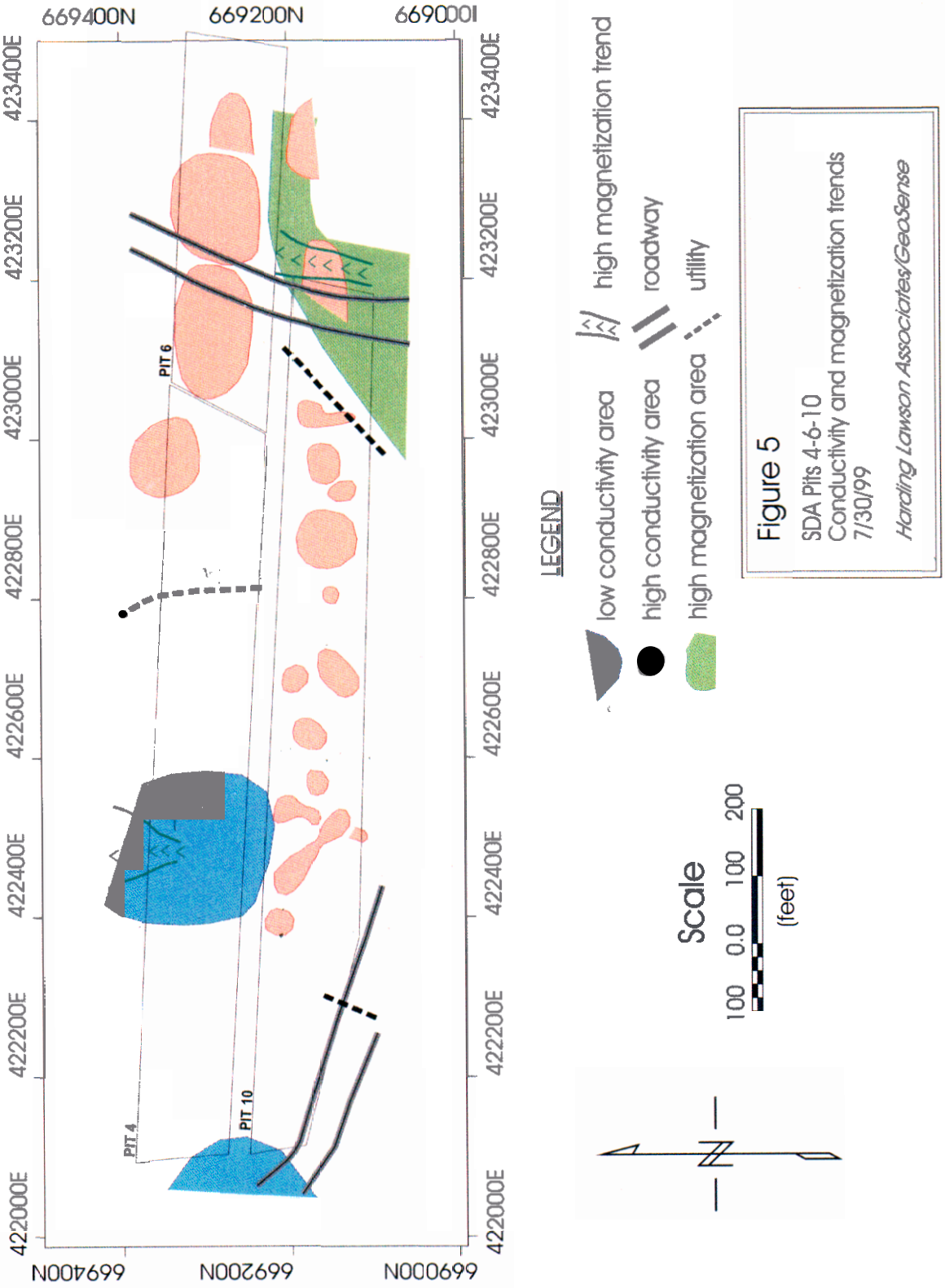

Figure 6. Depth to bedrock - seismic refraction.

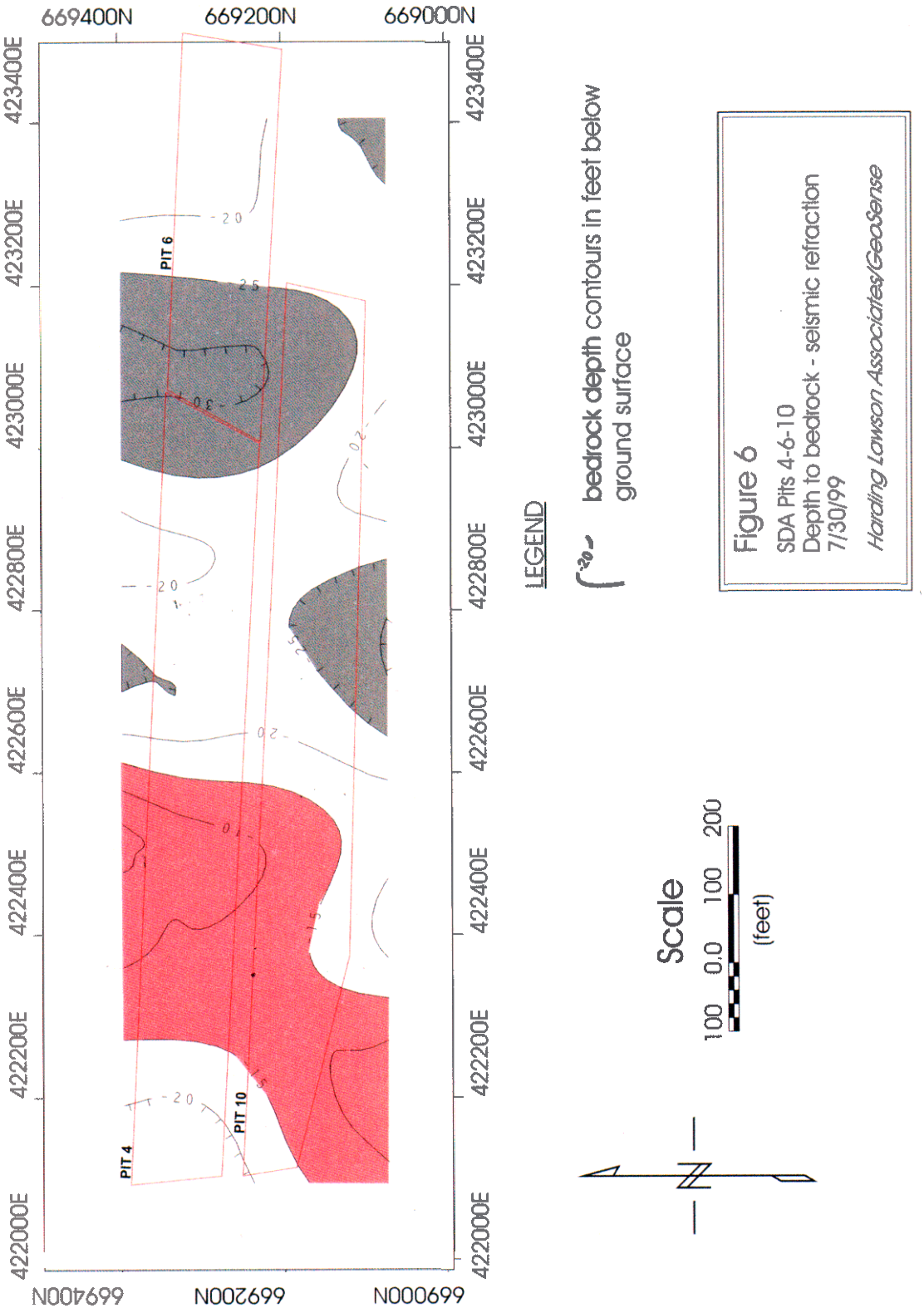

Figure 7. Depth to metallic waste.

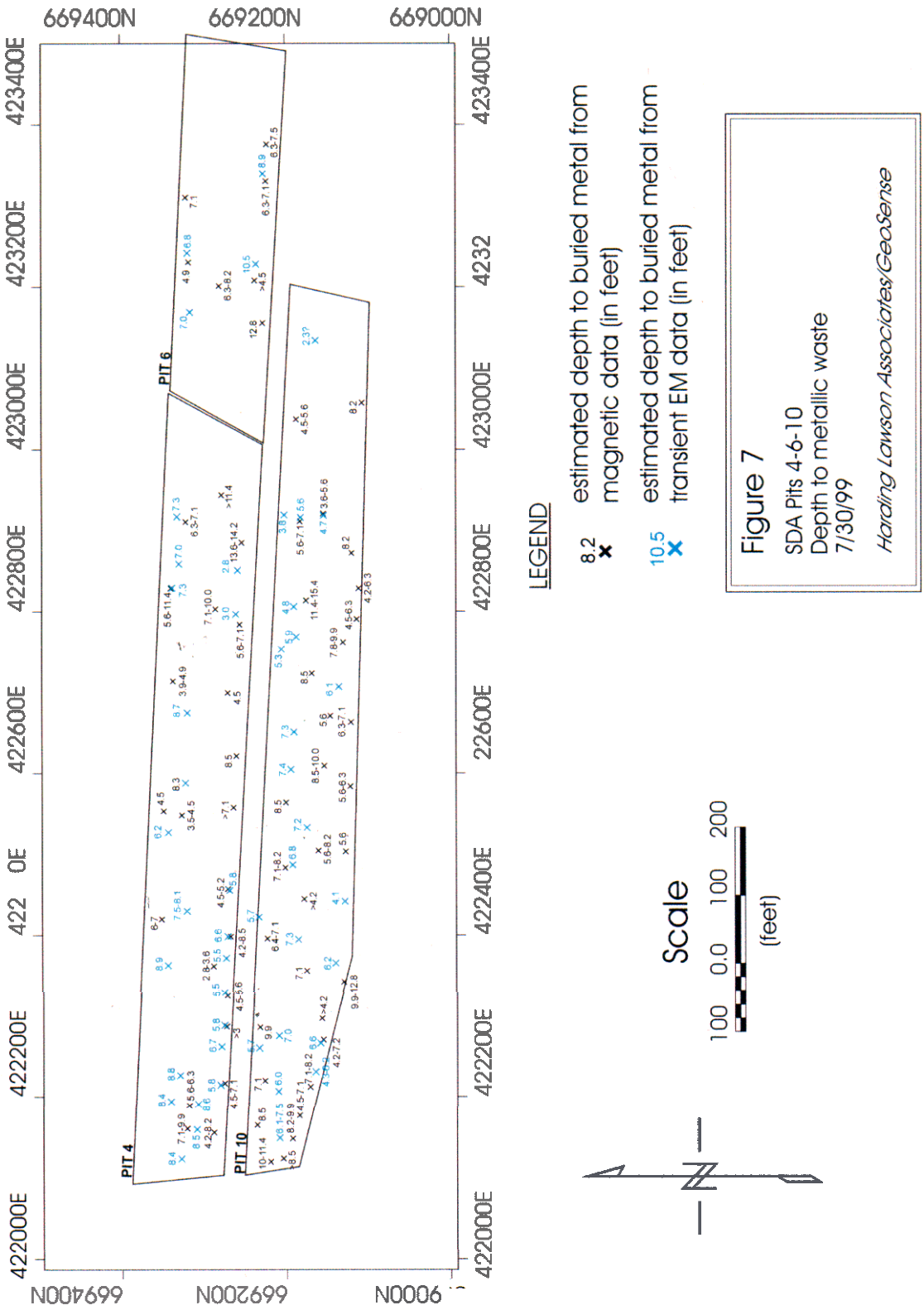

APPENDIX A - Map plates

Map displays for magnetic, transient EM and multi-frequency EM data are presented as follows.

Plate	Content
Plate 1	Total field magnetics
Plate 2	Vertical gradient magnetics
Plate 3	Transient EM - lower coil
Plate 4	Transient EM - differential
Plate 5	Multi-frequency EM - 450 Hz
Plate 6	Multi-frequency EM - 1590 Hz
Plate 7	Multi-frequency EM - 5610 Hz
Plate 8	Multi-frequency EM - 19950 Hz

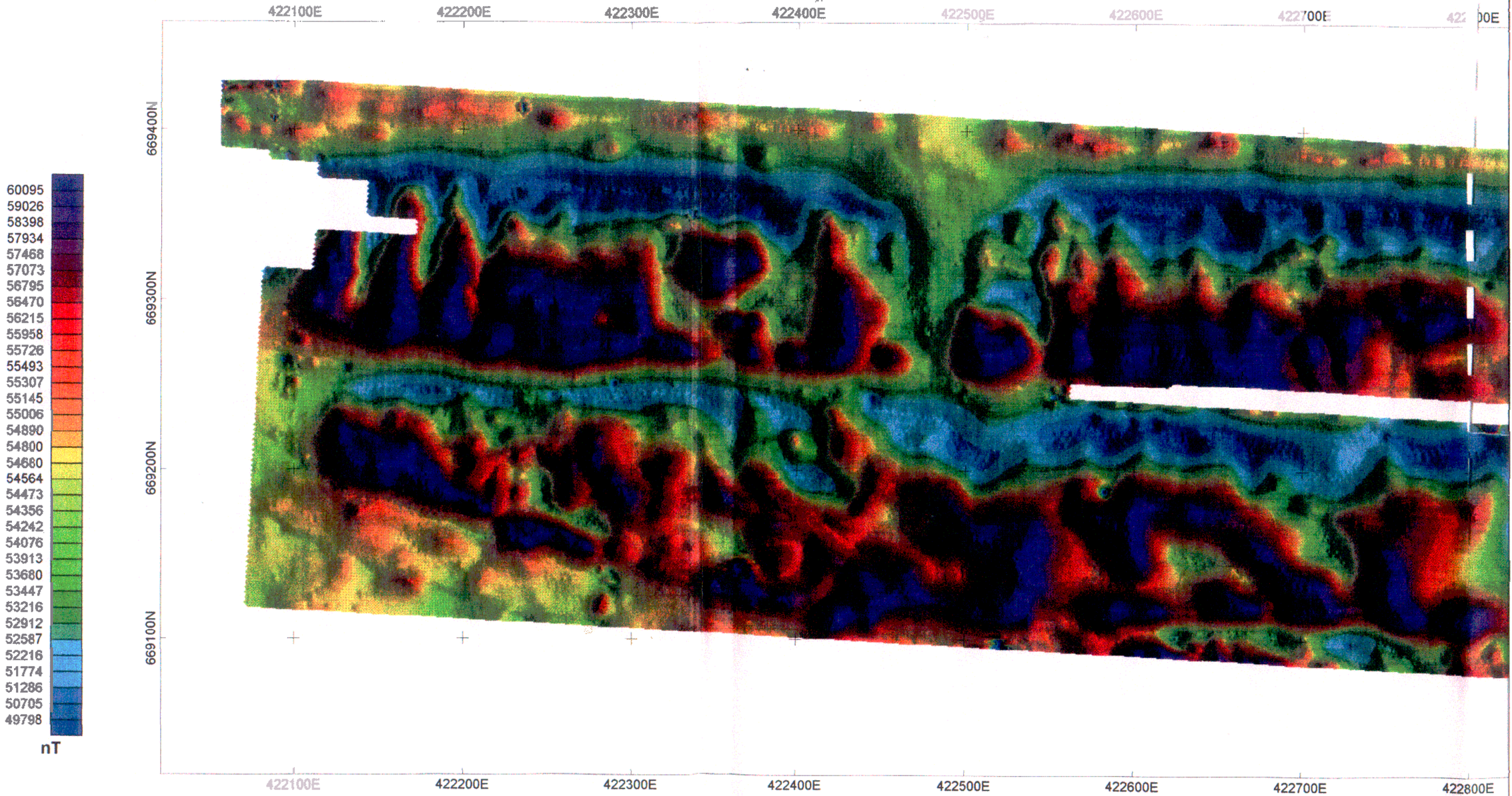
422100E
422200E
422300E
422400E
422500E
422600E
422700E
422800E
669400N
669300N
669200N
669100N
60095
59026
58398
57934
57468
57073
56795
56470
56215
55958
55726
55493
55307
55145
55006
54890
54800
54680
54564
54473
54356
54242
54076
53913
53680
53447
53216
52912
52587
52216
51774
51286
50705
49798
nT

422900E 423000E 423100E 423200E 423300E 423400E

669400N
669300N
669200N
669100N

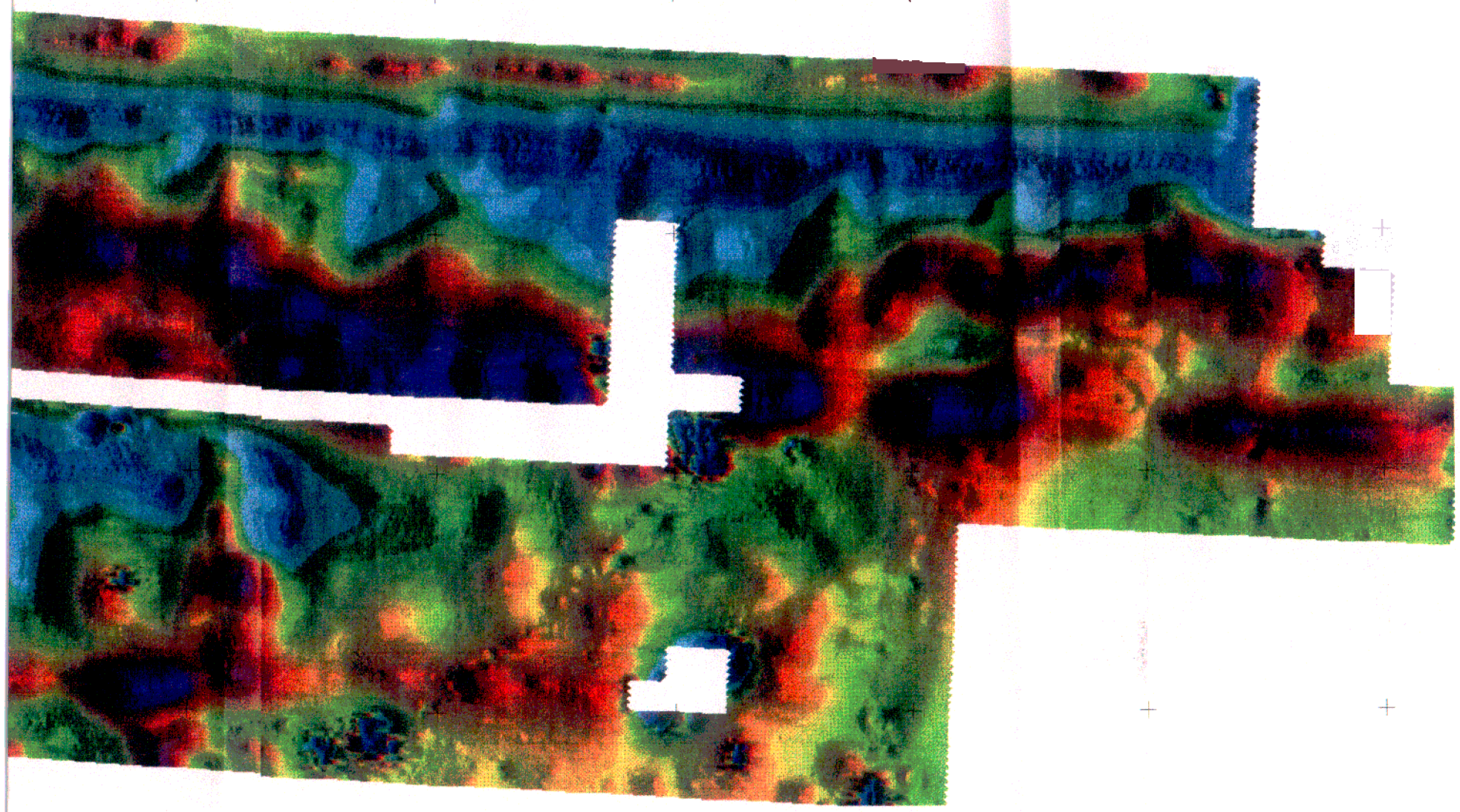

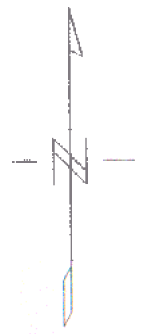

Scale 1:720

50 0.0 50 100 150

(feet)

422900E 423000E 423100E 423200E 423300E 423400E

LMITCO

SDA Pits 4-6-10
PLATE 1
Total Field Magnetics

Harding Lawson Associates/GeoSense